STAGING SCENARIOS FOR PROJECT-X*

N. Solyak[#], J-P. Carneiro, V. Lebedev, S. Nagaitsev, J.-F. Ostiguy, A. Saini, A. Vivoli, Y. Yakovlev
Fermilab, Batavia, IL 60510, U.S.A.

Abstract

Project-X is a high intensity proton source in development at Fermilab. At its heart is a linac based on superconducting technology comprising two distinct sections. The first one operates in CW mode and delivers beam with a flexible time structure to simultaneous experimental programs at 1 and 3 GeV. The second one operates in pulsed mode and accelerates a modest fraction (5%) of the beam from 3 GeV to 8 GeV for accumulation in the existing Main Injector complex. In an era of constrained budgets, construction in stages -with each stage capable of supporting worthy scientific programs - may be advantageous. Requirements for each program, coupled to the physical constraints imposed by the Fermilab site have led to a few possible scenarios, which are discussed in this contribution. In particular, we examine the implications of introducing bends in the linac at 1 and 3 GeV in terms of overall performance, flexibility and cost.

INTRODUCTION

Project-X is a proposed high intensity proton facility which can support many experiments simultaneously. In the present context of relative austerity for science, the current plan calls for building Project-X in stages. Each stage is associated with compelling scientific programs and in synergy with existing Fermilab infrastructure. After several iterations, the current "un-folded paper-clip" configuration was adopted as a baseline for the reference design report (see Fig.1). In addition, substantial modifications were introduced; they are discussed in details in [1, 2].
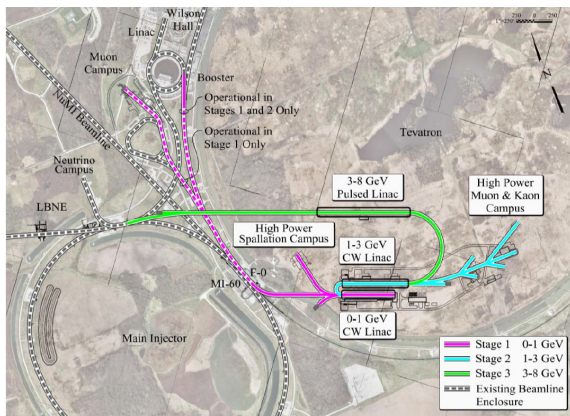

Figure 1: Layout of Project-X configuration.

Stage 1 involves the construction of a 1 GeV, 1 mA (average) CW linac providing beams to the existing Booster synchrotron, to a new muon campus (under

construction), and to a new 1 GeV experimental facility. The 1 GeV linac (shown in magenta) can be constructed with a minimal footprint while re-using existing beamlines (dashed lines). Stage 2 would double the average current in the 1 GeV linac and provide acceleration for half of the beam to 3 GeV into a second linac, with the 3 GeV beam aimed at a new high power muon and kaon campus located in the area enclosed by the old Tevatron. Stage 3 would further accelerate a small fraction of the 3 GeV beam up to 8 GeV into a pulsed superconducting linac for injection and accumulation into the existing recycler ring. Further acceleration can be provided after transfer into the Main Injector synchrotron. A detailed description of the staging approach for the Project-X facility is presented elsewhere [1, 3]. We shall focus here on the layout of a lattice designed to accommodate staging and discuss beam optics.
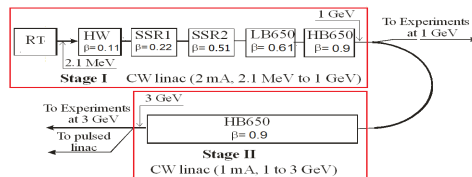

Figure 2: Acceleration scheme for various stages.

STAGE-I & II: CW LINAC DESIGN

One of the most challenging tasks for Project-X is to develop a robust design for the CW linac which has to provide high quality beam to various experiments simultaneously. At the completion of phase 2, the CW linac (Figure 2) will be used to accelerate H$^-$ ion beam from kinetic energy of 2.1 MeV up to 3 GeV. However, the success of Project-X is primarily dependent on reliable operation of the first stage, since most of the complexity lies at low energy when dynamics is not fully relativistic and space charge effects must be accounted for. The room temperature Front-End of the first stage consists of an ion source, a low energy beam transport section (LEBT), an RFQ and medium energy beam transport (MEBT). The ion source provides a nominal 5 mA, H- ion DC beam which is transported to RFQ through LEBT [4]. Next, a 162.5 MHz RFQ provides longitudinal bunching as well as acceleration up to an energy of 2.1 MeV. The RFQ is followed by the MEBT where the beam is chopped to obtain the time structure required to simultaneously support different experiments. Beyond the MEBT, the beam is accelerated from 2.1 MeV to 1 GeV in a CW linac. As shown in block diagram (Fig.2), the linac is divided into three sections on the basis of the cavities operating frequencies: (i) 162.5 MHz section, (ii) 325 MHz section and (iii) 650 MHz section. The first section uses half wave resonators to reach ~9

04 Hadron Accelerators

A17 High Intensity Accelerators

MeV. The second section uses two families of single spoke resonators (SSR1 and SSR2) to accelerate the beam from 9 MeV to 155 MeV. The last section uses two families of superconducting elliptical shape cavities, referred to as LB (β=0.61) & HB (β=0.9). While beam optics below 1 GeV is minimally affected by staging, the initial beam parameters, as well as the configuration of the cryomodules downstream of the MEBT have been updated. The changes provide additional longitudinal acceptance margin and were in part motivated by recent RFQ simulation results [4].

Acceleration of beam in 1-3 GeV linac (second stage) is performed using same HB 650 MHz elliptical cavities but modified cryomodule. RF transverse defocusing is less at high energy and it allows us to increase transverse focusing period which results in more cavities per cryomodule (8 vs. 6 in 1 GeV linac).

From the end of first stage linac, the beam is transported through a 180^0 turn-around bend to the second stage linac. A similar approach is used between the end of the second stage linac and the third stage pulsed linac. In the current baseline proposal, the two 180^0 turn-around bends are designed to be achromatic and isochronous to control bunch lengthening and emittance growth. Assuming that bending is restricted to the horizontal plane, achromaticity is achieved when the entries R_{16} and R_{26} of the turnaround transfer matrix vanish. We therefore demand that the dispersion η and its derivative vanish on both sides of the turnaround:

$$\eta(0) = \eta(L) = 0; \qquad \eta'(0) = \eta'(L) = 0; \qquad (1)$$

For a lattice constructed from N identical cells with (horizontal) transverse transfer matrix M, it can be shown that R_{16} and R_{26} vanish if $M^N = I$. The achromatic condition can therefore be satisfied by constructing the turnaround arc optics from N identical FODO cells in such a way that $N\cdot\phi_c = 2\pi\cdot k$; with k in an integer and ϕ_c the cell phase advance. To minimize the overall length, the field strength in each bending magnet should be as high as possible, but remain below a value that prevents excessive Lorentz stripping. To keep stripping losses < 0.1 W/m, the bending fields at 1 and 3 GeV should be respectively less than 0.27 T and 0.12 T.

Expressed as a constraint on the transfer matrix, isochrononicity is equivalent to demand that the condition

$$R_{56} = \frac{\partial z}{\partial \delta} = \left[-\int \frac{\eta(s)}{\rho(s)} ds + \frac{L}{\gamma^2} \right] = 0; \qquad (2)$$

be satisfied, where ρ is the bending radius and L is the total path length along the reference orbit. Since the dispersion generated in the bending magnets itself scales like $1/\rho$, the dispersion integral above scales like $1/\rho^2$ while L is proportional to ρ. This suggests that it is possible to choose ρ so as to make R_{56} vanish. In the presence of space charge, the single particle optics solution provides a good starting compromise, even though in that case achromaticity and isochronicity are no longer achieved and some emittance growth is unavoidable.
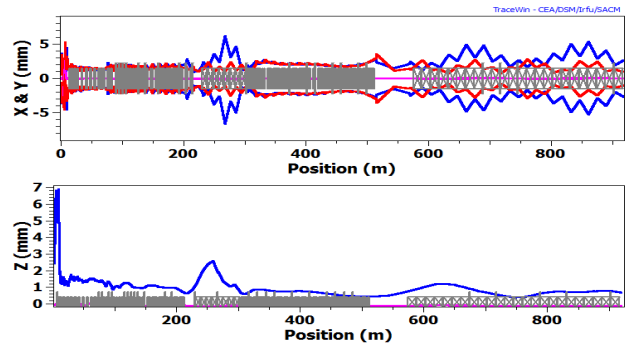

Figure 3: $1\times\sigma_{rms}$ beam envelopes. Top: transverse (x-blue, y-red). Bottom: longitudinal.

Figure 3 shows $1\sigma_{rms}$ beam envelopes for the complete CW linac (stage 1 + stage 2) using the code TRACEWIN. 10^6 macro-particles (6σ Gaussian distribution) are tracked, from the RFQ output to the exit of the 3 GeV bend.
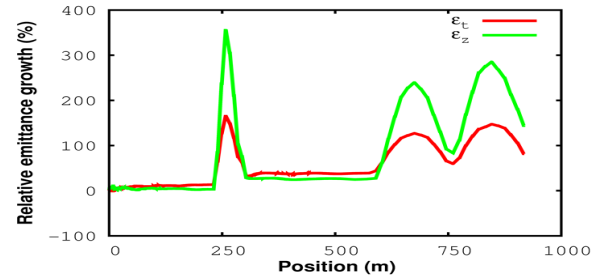

Figure 4: Relative emittance growth along the linac in longitudinal (green) and transverse (red) plane.

Figure 4 shows the relative transverse and longitudinal emittance growth along the linac. Normalized beam emittances (ϵ_x, ϵ_y and ϵ_z) at critical locations in the lattice are summarized in Table 1.

Table 1: Normalized Beam Emittance at the End of Critical Locations in Lattice

Location	ϵ_x π.mm mrad	ϵ_y π.mm mrad	ϵ_z π.mm mrad
Initial	0.21	0.21	0.28
1 GeV linac	0.23	0.24	0.29
1 GeV bend	0.316	0.247	0.36
3 GeV linac	0.332	0.25	0.35
3 GeV bend	0.516	0.28	0.68

It should be noticed that emittance dilution in the horizontal and longitudinal plane is dominated by the turnarounds. Due to a lower allowed bending field, the 3 GeV bend is significantly longer than its 1 GeV counterpart (350 m vs 70 m). Although space charge forces are lower at 3 GeV, they act for a longer period.

Studies have been performed to analyse the robustness of lattice. Machine acceptances were calculated at different locations along the linac. In general, a larger

acceptance results in better tolerance against imperfections. Typically, in a superconducting ion machine with high acceleration efficiency, the longitudinal margin is more critical than the transverse.

Fig. 5 shows the longitudinal acceptance at different locations, in different colors, along the linac. The input distribution (pale yellow) was tracked from the MEBT output. It is found that the linac longitudinal acceptance is primarily limited by the SSR2 section and is large enough to comfortably accommodate a 6σ Gaussian beam, shown in black.
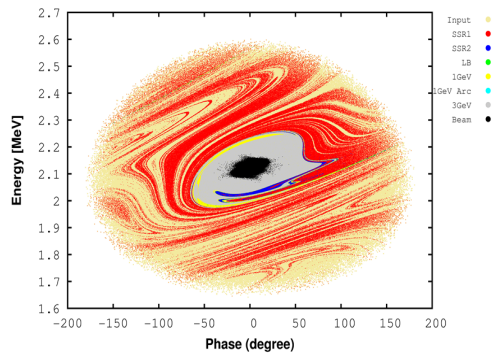

Figure 5: Longitudinal acceptance of baseline design at different locations along the CW linac.

Studies have also been performed, using the code TRACK to understand the sensitivity of the baseline lattice against static misalignments and dynamic RF jitter (field amplitude and RF phase). Static transverse misalignments are uniformly distributed with maximum amplitude δ_{xy}. The dynamic RF errors have a Gaussian distribution truncated at 3σ.
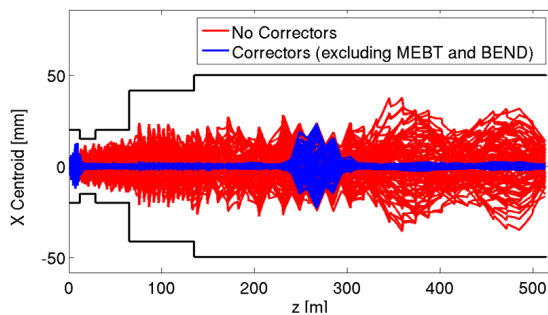

Figure 6: TRACK simulations of corrected (blue)/ uncorrected (red) horizontal beam centroid along linac.

Figure 6 shows results obtained for the set of errors δ_{xy} = 1 mm (solenoids and cavities), δ_{xy} = 0.5 mm + 5 mrad roll for quadrupoles. The dynamic RF jitter was set to 0.5^0+0.5% in the HWR, SSR1 and SSR2 sections, 1^0+1% in the LB and HB sections. A correction scheme was applied assuming one corrector and a BPM per solenoid and quadrupole doublet. The resolution and the offset in position of the BPMs are 30μm and 1 mm respectively. No beam losses are observed after the correction was applied. No

imperfections (static and dynamic) were included in MEBT and 1 GeV bend section for this study.
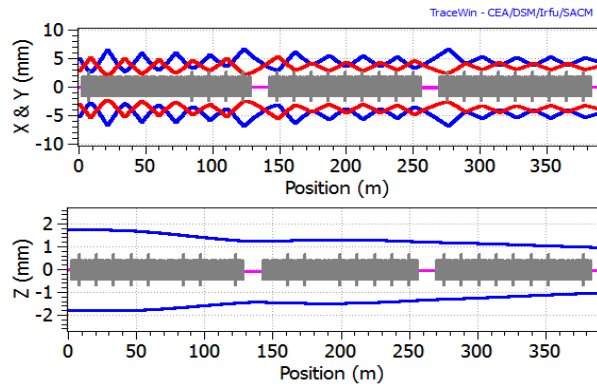
STAGE-III: PULSED LINAC DESIGN

Figure 7: $3\sigma_{rms}$ beam envelopes. Top: transverse (*x*-blue, *y*-red). Bottom: longitudinal.

The third and final phase of Project-X involves the addition of a 3 GeV turn-around and an SRF 3-8 GeV, 1 mA, pulsed linac. While staging does not affect the required number of cryomodules, the beam optics was retuned to accommodate the larger beam emittance coming out of the 3 GeV bend. The baseline lattice [1] for the pulsed linac is segmented into three cryo-strings composed of 10, 9 and 9 cryomodules respectively. Cryo-strings are separated from each other by room temperature sections which will be used for beam collimation, diagnostics and maintenance. Fig. 7 shows beam envelopes along the linac. No significant emittance growth occurs in the pulsed linac.

CONCLUSION

We now have a complete lattice design incorporating all the necessary changes for a staged Project-X. Preliminary beam dynamics studies show that the basic performance and sensitivity to errors in a staged scenario is similar to what was demonstrated earlier for a conventional straight layout. The main impact of staging is the emittance increase associated with the turnarounds. In spite of this, beam quality meets the requirements set for the project.

REFERENCES

[1] "Project-X reference design report", Fermilab, USA 2013.
[2] N. Solyak, et al, in proceedings IPAC 2013, THPWO092.
[3] R. Tschirhart et al, "Staging Opportunities at Project X", IPAC 2013.
[4] J.F. Ostiguy, et al, "PXIE End-to-end Simulations", IPAC 2013.